

Supplementary Data

In-situ constructing C₃N₅ nanosheets/Bi₂WO₆ nanodots S-scheme heterojunction with enhanced structural defects for efficiently photocatalytic removal of tetracycline and Cr(VI)

Shijie Li^{a,b*}, Mingjie Cai^{a,b}, Yanping Liu^{a,b}, Junlei Zhang^{c*}, Chunchun Wang^{a,b}, Shaohong Zang^{a,b}, Youji Li^d, Peng Zhang^e, Xin Li^{f*}

^a Key Laboratory of Health Risk Factors for Seafood of Zhejiang Province, National Engineering Research Center for Marine Aquaculture, College of Marine Science and Technology, Zhejiang Ocean University, Zhoushan, Zhejiang Province, 316022, China.

^b Institute of Innovation & Application, Zhejiang Ocean University, Zhoushan, Zhejiang Province, 316022, China.

^c State Key Laboratory of Solidification Processing, School of Materials Science and Engineering, Northwestern Polytechnical University, Xi'an 710072, PR China

^d College of Chemistry and Chemical Engineering, Jishou University, Jishou, Hunan 416000, PR China

^e State Center for International Cooperation on Designer Low-Carbon & Environmental Materials (CDLCEM), School of Materials Science and Engineering, Zhengzhou University, 100 Kexue Avenue, Zhengzhou, 45001, PR China

^f Institute of Biomass Engineering, Key Laboratory of Energy Plants Resource and Utilization, Ministry of Agriculture and Rural Affairs, South China Agricultural University, Guangzhou 510642, P.R. China

* Email: lishijie@zjou.edu.cn (S.J. Li); junlei@nwpu.edu.cn (L.J. Zhang); xinli@scau.edu.cn (X. Li)

2. Experimental

2.1. Catalysts characterization

Powder X-ray diffraction (XRD) characterizations were completed on a Rigaku MiniFlex 600 diffractometer with CuK α radiation (0.154 nm). X-ray photoelectron spectroscopy (XPS) equipped with a Thermo Fisher Scientific Escalab 250Xi spectrometer was utilized to uncover the bonding information. The electron paramagnetic resonance (EPR) spectra were determined with a Bruker EMXplus EPR spectrometer. The morphology and elemental composition were determined with a scanning electron microscopy (SEM, Hitachi S-4800), transmission electron microscopy (TEM, Hitachi H600), and an energy dispersive X-ray spectroscopy system (EDX). UV-vis diffuse reflectance spectra (UV-vis DRS) were

acquired on a SHIMADZU UV-2600 UV-vis spectrophotometer coupled with the integrating sphere. The steady and time-resolved photoluminescence (PL) spectra were acquired by utilizing an Edinburgh FL/FSTCSPC920 fluorescence spectrophotometer. The Brunauer–Emmett–Teller (BET) specific surface areas were analyzed by using a Quantachrome Autosorb-iQ-2MP system. The transient photocurrent responses (TPR), electrochemical impedance spectra (EIS) and Mott-Schottky (MS) plots were obtained on a CHI660E electrochemical workstation in a three-electrode configuration utilizing Pt foil, Ag/AgCl and the fluorine-doped tin oxide (FTO) coated with samples as the opposite electrode, reference electrode, and the working electrode, respectively. The electrochemical measurements were performed in a 0.5 mol/L Na₂SO₄ aqueous solution. The electronic structures of the samples were analyzed by CASTEP codes (GGA and PBE). Electron spin resonance (ESR) analysis by utilizing Bruker ESR 300E spectrometer was performed to probe the generation of •OH and O₂^{•-} species, in which 5,5-dimethyl-1-pyrroline-N-oxide (DMPO) was functioned as a spin trap.

2.2. Degradation intermediates identification

The TC degradation intermediates were monitored using a Ultimate 3000 UHPLC–Q instrument coupled to a time-of-flight mass spectrometer (HPLC-TOF–MS) system (Bruker solanX 70, Germany) equipped with an electrospray ionization source (ESI) in the positive

ion mode. HPLC separation was conducted on a Waters BEH C18 column. The mobile phase was composed of acetonitrile and formic acid (0.1%) and the flow rate was 0.3 mL/min. The injection volume of specimen was 10 μ L. The acquisition mode for determination was single MS, while source accumulation, ion accumulation time and flight time for decision were 0.100, 0.500 and 0.001sec, respectively.

Figures

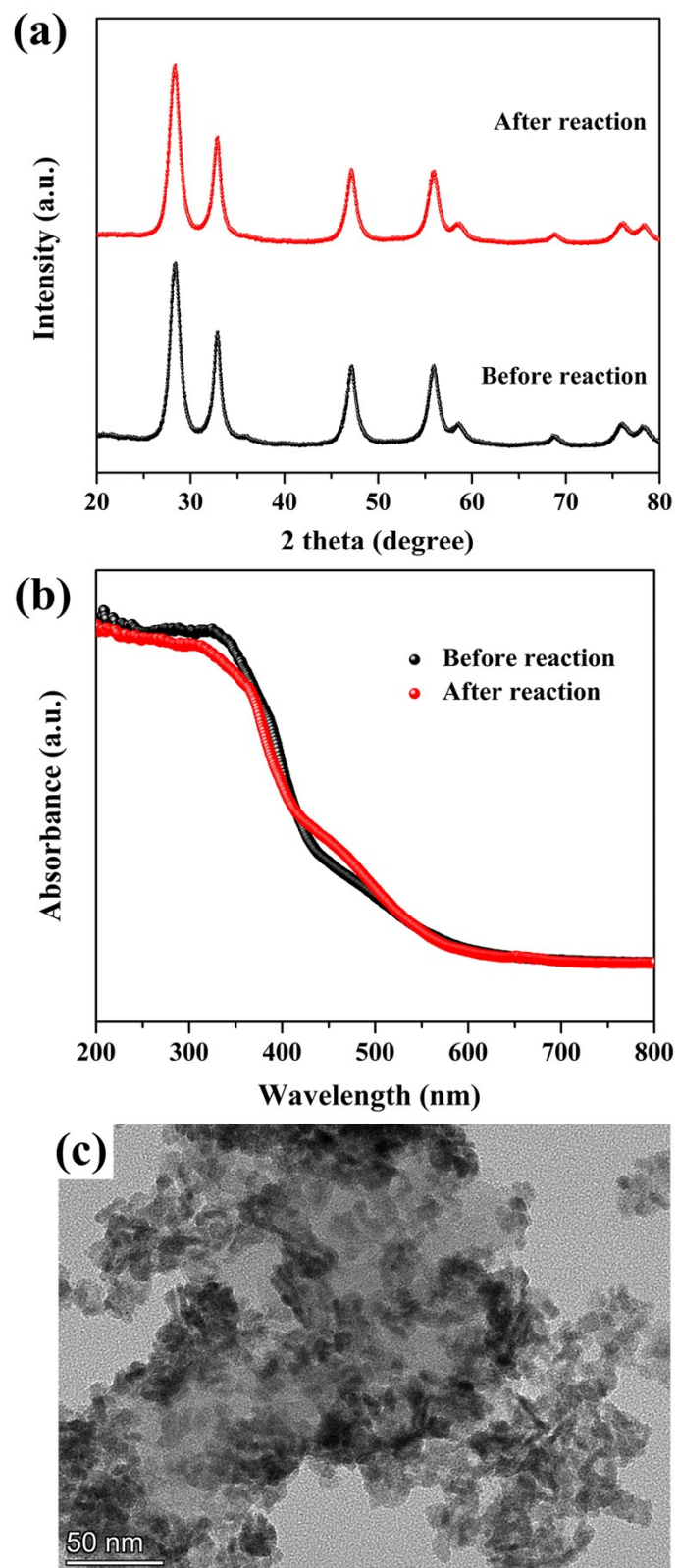


Figure S1 (a) XRD patterns and (b) DRS of the fresh and used 10CN/BWO; (c) TEM image of the used 10CN/BWO.

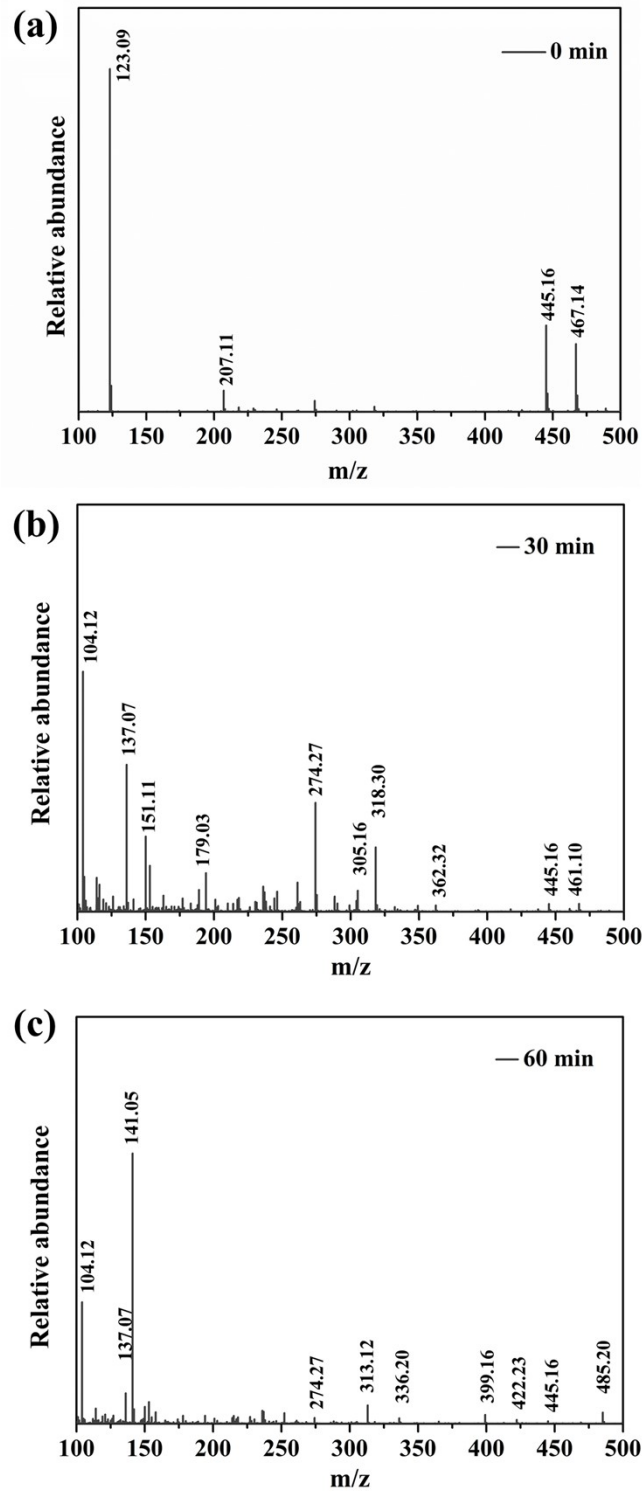


Figure S2 The Maldi-TOF-MS of the TC degradation of 0, 30, and 60 min by 10CN/BWO

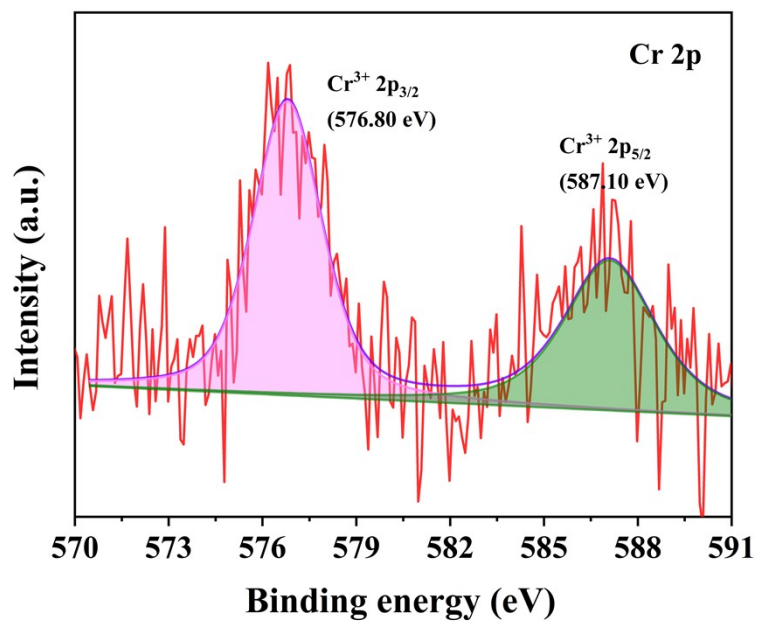


Figure S3 XPS spectrum of the recycled 10CN/BWO: Cr 2p.

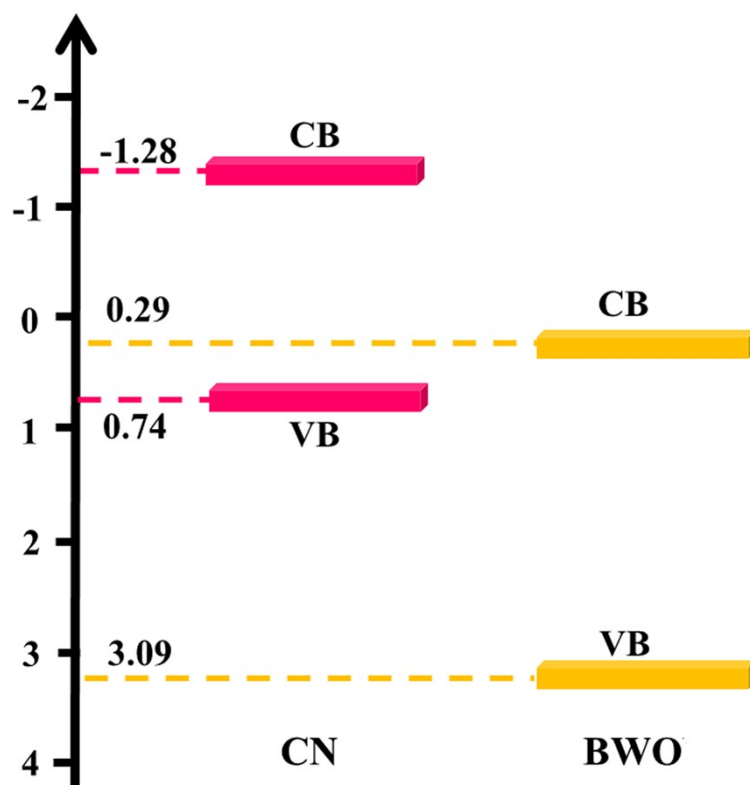


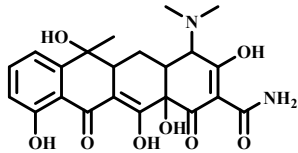
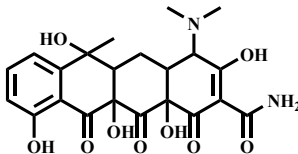
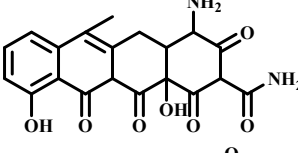
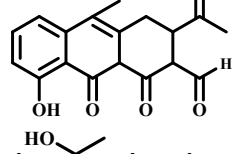
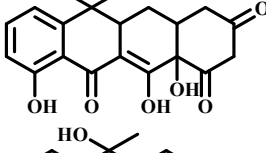
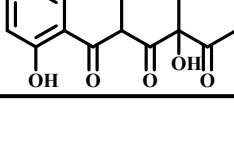
Figure S4 The band structures of CN and BWO.

Tables

Table S1 The parameters of the actual water body

Water bodies	Ca ²⁺ (mg L ⁻¹)	Cl ⁻ (mg L ⁻¹)	NO ₃ ⁻ (mg L ⁻¹)	COD (mg L ⁻¹)	TOC (mg L ⁻¹)
Tap water	4.26	21.64	2.26	1.57	1.69
River water	48.91	38.74	7.75	9.56	8.87

Table S2 Possible intermediates for TC degradation using 10CN/BWO as the catalyst under visible-light irradiation.

Substance	Formula	m/z	Potential structure
Tetracycline (TC)	C ₂₂ H ₂₄ O ₈ N ₂	445.16	
P1	C ₂₂ H ₂₄ O ₉ N ₂	461.10	
P2	C ₂₀ H ₁₈ O ₇ N ₂	399.16	
P3	C ₁₈ H ₁₆ O ₅	313.12	
P4	C ₁₉ H ₁₈ O ₇	362.32	
P5	C ₁₇ H ₁₈ O ₆	318.30	

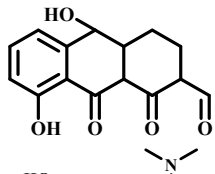
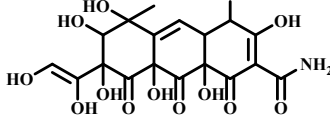
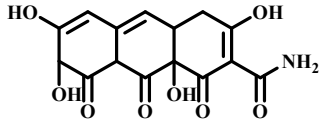
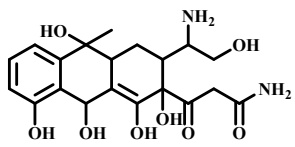
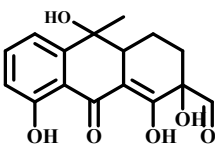
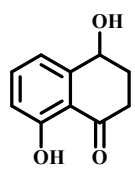
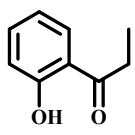
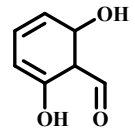
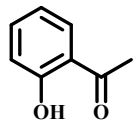
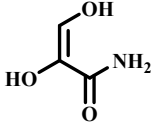
P6	$C_{15}H_{14}O_5$	274.27	
P7	$C_{20}H_{24}O_{12}N_2$	485.20	
P8	$C_{15}H_{13}O_8N$	336.20	
P9	$C_{20}H_{26}O_8N_2$	422.23	
P10	$C_{16}H_{16}O_6$	305.16	
P11	$C_{10}H_{10}O_3$	179.03	
P12	$C_9H_{10}O_2$	151.11	
P13	$C_7H_8O_3$	141.05	
P14	$C_8H_8O_2$	137.07	
P15	$C_3H_5O_3N$	104.12	

Table S3 Toxicity prediction values and results of TC and its intermediates calculated by TEST.

Substance	Acute toxicity	Developmental toxicity		Mutagenicity	
	Daphnia magna LC ₅₀ (48 h) (mg/L)	Predicted value	Predicted result	Predicted value	Predicted result
TC	8.70	0.89	Developmental toxicant	0.56	Positive

P1	21.43	0.88	Developmental toxicant	0.56	Positive
P2	17.91	1.17	Developmental toxicant	0.56	Positive
P3	24.14	0.97	Developmental toxicant	0.46	Negative
P4	20.34	0.84	Developmental toxicant	0.62	Positive
P5	34.83	0.81	Developmental toxicant	0.51	Positive
P6	36.39	1.01	Developmental toxicant	0.33	Negative
P7	275.94	0.65	Developmental toxicant	0.57	Positive
P8	61.76	0.85	Developmental toxicant	0.55	Positive
P9	7.87	0.59	Developmental toxicant	0.54	Positive
P10	9.79	0.77	Developmental toxicant	0.57	Positive
P11	17.60	0.66	Developmental toxicant	0.48	Negative
P12	6.63	0.48	Developmental non-toxicant	0.43	Negative
P13	19.77	0.22	Developmental non-toxicant	0.11	Negative
P14	20.38	0.41	Developmental non-toxicant	0.09	Negative
P15	652.65	0.43	Developmental non-toxicant	0.16	Negative
